energies

MDPI

Article

Use of Tanδ and Partial Discharge for Evaluating the Cable Termination Assembly

Cihat Cagdas Uydur [1,*] and Oktay Arikan [2]

[1] Technical Sciences Vocational School, Trakya University, Edirne 22020, Turkey
[2] Department of Electrical Engineering, Yildiz Technical University, Istanbul 34220, Turkey; oarikan@yildiz.edu.tr
* Correspondence: ccagdasuydur@trakya.edu.tr

Received: 8 September 2020; Accepted: 8 October 2020; Published: 12 October 2020



Abstract: It is known that the failure of cable terminations causes power outages and impairs system quality and continuity. Besides, serious economic losses on both the distribution and consumer sides occur. In this study, the dielectric behavior of the cable and the faults caused by the defects in the cable termination under overvoltage has been examined. As test samples, 12 kV XLPE insulated cable is used and they were aged at three ($3*U_0$) and five ($5*U_0$) times the rated voltage. After each aging cycle, dielectric parameters of the cable were measured by an OMIRCRON CPC100/CPTD1 device, and the partial discharge (PD) was measured by an OMICRON MPD600 device. In the measurements, it was observed that the cable was broken down at different aging cycle numbers as a result of defects in the cable termination due to weak workmanship. As a result of the measurements, it is concluded that defects in the cable termination give information about the increase in the probability of failure and the decrease of the cable lifetime. Consequently, it is concluded that fine workmanship and timely maintenance of cable terminations prevent the system from unwanted power outages and economic losses.

Keywords: aging; cable termination; dissipation factor; partial discharge; XLPE cable

1. Introduction

Considering the devices and equipment used in medium voltage (MV) distribution systems, power cables are one of the most basic elements and form the main structure of the electrical network for providing energy transmission; they carry energy, their investments are expensive, and if they fail, energy cuts, deterioration of power quality and continuity, and serious economic losses arise on both the distribution and the consumer side [1,2]. For this reason, it is of great importance that MV cables are operated reliably/without fail during their operation which provides a longer lifetime. To achieve this, dielectric diagnostic tests must be performed on cable components at certain periods [3]. The main purpose of these tests is to determine the effects of nominal operating conditions and the stresses caused by overvoltage and impulse voltage on the cable and cable termination.

In recent years, studies using various aging techniques have been carried out to investigate the electrical effects that underground cables can be exposed to. These aging techniques can be summarized as overvoltage, a voltage level higher than the rated voltage of the cable, switching/lightning impulse voltages, and finally thermal aging by exposing the insulating material of the cable to high temperatures [4,5]. In aging procedures of using overvoltage, three and four times the rated voltage (U_0) is applied to the cable and partial discharge (PD) and dissipation factor (tanδ) diagnostic methods are used; negative results have been reported [6,7]. The $2*U_0$ overvoltage and thermal aging methods have been used in studies for comparing multiple aging methods [8,9]. Publications that prove the sensitivity of PD measurement in the impulse voltage and aging process and evaluate the results

with the help of life calculations have also taken place in the literature [10,11]. Additionally, aging processes have been performed on different insulation materials and the insulation materials have been classified by using PD measurement results [12]. There are also studies performed in which life estimations are made by examining PD measurements. Knenicky et al. stated that due to termination in the cable samples, life prediction is quite difficult and can give misleading results [13]. In a study conducted by Eigner and Rethmeier in 2016, the authors discussed the issue that more sensitive PD measurements can be made to detect the installation errors in the cable accessories and the faults. It is stated that PD measurement gives information about the assembly quality [14]. Xu et al. investigated the effect of defects on PD in the cable that may result during cable termination assembly. In the study, a 50-kV amplitude switching pulse (250/2500 μs) is applied to the cable samples and hazards arising from different assembly defects that may arise during operation have been demonstrated [15]. In the study by Wu et al., PD measurements on an XLPE insulated test samples were carried out to examine the dielectric behavior of cable joints for transient impulse. As a result, it was stated that defects occurring during assembly change PD formation [16]. Ghaderi et al. also measured the tanδ by heating the cable joints and examined the dielectric behavior of the cable joints. By comparing with the values obtained from the manufacturer, he stated that the cable joint is adversely affected by the temperature and possible assembly errors can lead to bad results [17,18].

In this study, dielectric behavior of the cable and the faults caused by the defects that may occur in the termination of the cable under overvoltage has been examined. Four test samples (12/20.8-kV XLPE insulated cable) were used and were aged with overvoltage using three times ($3*U_0$) and five times ($5*U_0$) the rated voltage in the Yildiz Technical University High Voltage Laboratory. Aging processes were carried out by applying overvoltage to the cable insulation at 15 minutes intervals. After each aging process, dielectric parameters of the cable (dissipation factor (tanδ), dielectric losses (P_k), and dielectric constant (ε)) were measured with the OMIRCRON CPC100/CPTD1 device and partial discharge (PD) was measured with the OMICRON MPD600 device. The results obtained are presented by analyzing the dielectric characteristic of the cable by applying overvoltage. In addition, the effects of workmanship errors for cable termination on measurements are stated. According to the measurement results, it was observed that the failure probability of the cable system increased due to overvoltage rises and also cable lifetime was shortened. Examining the results obtained in detail is quite beneficial in terms of dielectric performance and will contribute to preventing energy cuts and economic losses.

2. Typical Installation and Assembly Defects of Cable Terminations

In the distribution system, during the transportation or assembly of the underground cable, unwanted defects and deteriorations may occur in the cable, cable ends, and joints which can lead to serious failures. The way the fault occurred may vary depending on system voltage and quality of cable termination workmanship during installation. The characteristics of the workmanship error can play an active role in determining the initial conditions for failure in cable terminations and joints. As a result, the electric field distribution within the cable insulation becomes non-uniform. Non-uniform electric field distribution leads to an increase in PDs and the insulation properties of the material deteriorate in a shorter time [19].

2.1. Installation of Cable Terminations

In cable systems, cable termination installation is of great importance for steady operation. It is necessary to prevent possible errors that may happen during installation in order to ensure system reliability. Figure 1 shows a standard cable termination. Examining the details and assembly steps in cable termination will help to understand this situation.

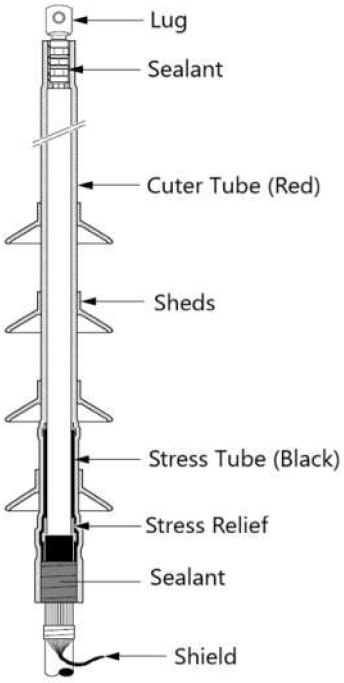


Figure 1. Parts of cable termination [20].

During the termination assembly, the outer sheath of the cable should be properly stripped, the shield of the cable should be folded so as not to form a sharp edge and the sealant should be mounted in a way to form a homogeneous structure. The most important element of the termination assembly defects is the semiconductor sheath on the insulator surface. In addition, the factors determine the quality of workmanship by installing the stress control tube in the proper position and correcting the thermal shrinkage. Sealant should be used so that there is no gap between the edge of the cable lug and the cable insulator. Finally, the heat shrinkage process of the outer sheath should be done at a distance that will not damage the sheath and without leaving foreign matter on the surface by wrapping the cable insulator completely. The termination assembly must be completed perfectly by adding an appropriate number of sheds to the voltage [20].

2.2. *Assembly Defects of Cable Terminations*

In order for the termination assembly to be accepted as flawless, many process steps should be performed properly. The slightest error at any stage can cause the termination assembly to be defective and lead to non-uniform electric field distribution. Possible defects that may occur in the cable termination are shown in Figure 2.

While the outer sheath of the cable is being removed during the termination assembly, a mechanical deformation (cut, scratch, crush, etc.) may occur on the insulator surface resulting in the deterioration in equipotential distribution and increase in electrical stress. The rough surface may also occur during the stripping of the semiconductor sheath. The voids and notches on the insulation surface due to improper application cause the electric field distribution to increase. In addition, semiconductor sheath pieces remaining on the insulator surface may constitute weak points and cause incorrect measurement results. At the end of the stripping process, the misapplication of the stress relief material between the semiconductor and insulation surface will trigger other faults such as PD and breakdown. The stress control tube will lose its electrical properties due to overheating and becomes one of the weakest points. The most important defect that can occur in the cable lug and cable shield assembly is the incorrect positioning of the lug or shield causing sharp edges. The jagged edges may cause PD resulting in other cable terminations to be heated, which will adversely affect operating conditions.

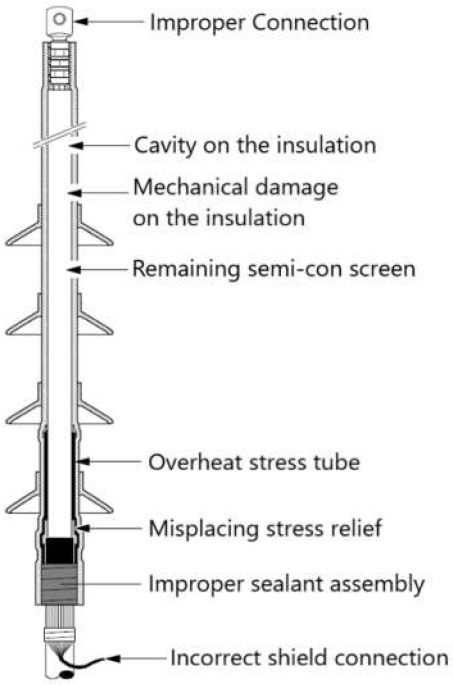


Figure 2. Defects of cable termination [20].

It is known that most of the failures occurring in distribution systems are related to cable terminations and joints. Cable termination and joint failures generally take place due to poor workmanship during installation and assembly. Poor workmanship disrupts the electric field distribution in the cable termination and causes high electric field formation. It leads to increased PDs in the voids and the material properties deteriorate rapidly. While some workmanship errors cause failures during acceptance tests, others lead to failures in the operation of the cable [19,20].

3. Theoretical Background

Underground cables used in energy distribution systems deteriorate due to high electrical and mechanical stresses during the operation. There are many dielectric diagnostic methods to determine the effects of these voltages on the cable insulation. The most important one of these methods is the tanδ and PD measurements.

3.1. Dissipation Factor (tanδ)

Dielectric materials are used in electrical equipment for insulation purposes. When a voltage is applied, a potential difference to earth is created and an electric field originates in the insulation material (dielectric). Due to the potential difference, a capacitive current flows through the dielectric material [21]. This current will cause a loss in the dielectric material. In an ideal dielectric material, this loss corresponds to reactive power, while in the actual dielectric material it corresponds to reactive and active power. Active power loss, which manifests itself in the form of heat, is called dielectric loss as seen in Figure 3 [22].

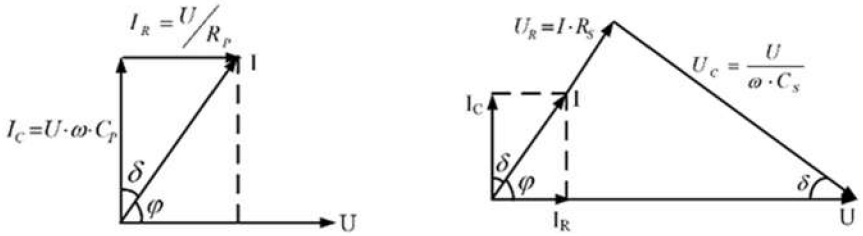
Here, C represents the capacity of the dielectric material, and R represents the dielectric losses in the insulation material. Accordingly, the current passing through the dielectric material has active (I_R) and reactive (I_C) components. In other words, tanδ expresses the ratio of the losses in the dielectric material. The tanδ is calculated by dividing the active component of the current drawn by the reactive

component. The analytical methods for calculating the tanδ and P_k for a parallel equivalent circuit model are stated in Equations (1) and (2) [22].

$$\tan\delta = \frac{I_R}{I_C} = \frac{U/R}{U/1/\omega \cdot C} = \frac{1}{\omega \cdot R \cdot C} \quad (1)$$

$$P_k = \omega \cdot C \cdot U^2 \cdot \tan\delta \quad (2)$$

In the above equations, C is the capacitance (F), R is the resistance (Ω), U is the voltage (V), ω is the angular frequency (rad/s) and f is the frequency (Hz).



(**a**) (**b**)

Figure 3. Phasor diagrams of dielectric material: (**a**) parallel and (**b**) series.

3.2. Partial Discharge (PD)

According to the IEC standard, PD is referred to as "one type of electric discharge that does not completely bridge the insulation between electrodes" [23]. Although PD can be literally used to describe the discharges in all environments, its usage in the solid or liquid dielectrics is generally restrained to those occurring in voids or cavities.

The voids are either filled with gas or liquid that mostly occur during the cross-linking and extruding process. A parallel-capacitor model can help to explain the initiation of PD. The equivalent circuit is used to evaluate the fundamental quantities related to a PD pulse is shown in Figure 4 [24]. This circuit consists of two electrodes, A and B, and a cavity separated by solid or liquid dielectric materials.

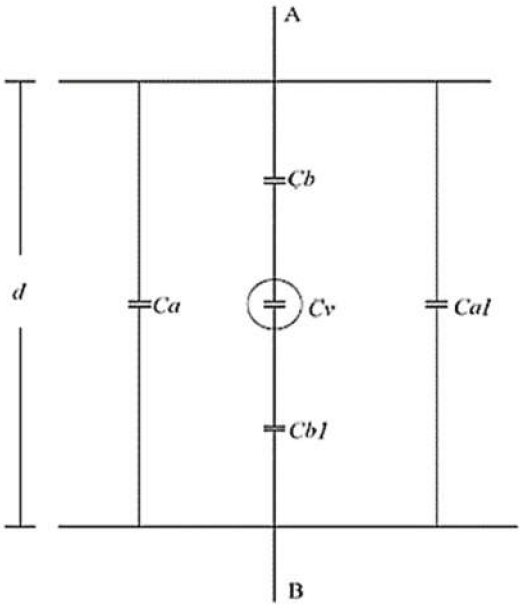


Figure 4. Equivalent circuit of PD [24].

C_b and C_{b1} are capacitances in the solid insulation area in series with the void, C_v represents the void while C_a and C_{a1} are the remaining capacitances of the dielectric. In the below Equations (3) and (4), d is the separation of electrodes (m), D_x is the width of the void (m), ε_r relative permittivity, E_a is the electrical field strength (V/m), and E_{vb} is the breakdown strength of the gas in the void (V/m).

$$P_k = \omega \cdot C \cdot U^2 \cdot \tan\delta \tag{3}$$

$$V_v = \frac{V_a}{1 + \frac{1}{\varepsilon_r}\left(\frac{d}{D_x} - 1\right)} \tag{4}$$

The electrical field strength across the void (E_v) equals:

$$E_v = E_a . \frac{d}{D_x \cdot \left(1 + \frac{1}{\varepsilon_r}\left(\frac{d}{D_x} - 1\right)\right)} \tag{5}$$

It can be noted that electrical stress inside the void is larger than the immediate insulation since $D_x << d$ and ε_r is greater than 1 in most cases. This makes the gas within the cavity responsible for the breakdown when the usual operating conditions are not adequate [25].

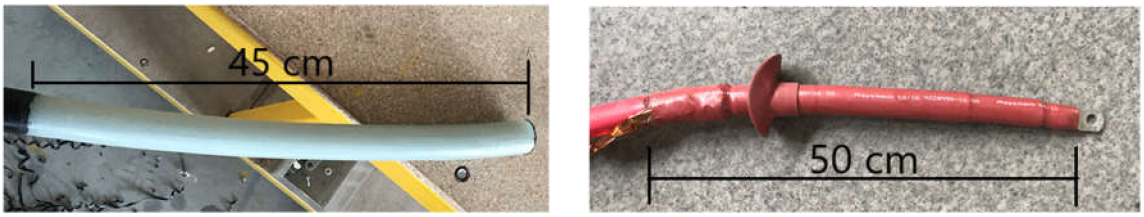
It is noted that the voltage across the dielectric material at which discharge action will start within the void (V_{ai}) is given in Equation (6).

$$V_{ai} = E_{vb} \cdot D_x \cdot \left(1 + \frac{1}{\varepsilon_r}\left(\frac{d}{D_x} - 1\right)\right) \tag{6}$$

4. Experimental Setup

In the measurements, medium voltage cables (1×25 mm^2—12/20.8 kV NA2XSY) were used. They were in the form of a stranded aluminum conductor, inner semiconductor, XLPE insulation, outer semiconductor, semiconductor tape, copper screen, polyester tape, and PVC outer sheath.

Before tests, to prevent partial and surface discharges and to regulate electric field distribution, cable termination was fitted. For assembling cable terminations, cable samples were cut to 5 m long and then both ends were prepared as shown in Figure 5.



(**a**) (**b**)

Figure 5. Preparation of cable samples: (**a**) stripping of the semiconductor layer and (**b**) measured cable sample.

In order to investigate the effects of aging in cables and cable terminations, an overvoltage aging process was applied. In the literature [6–9], aging cycle times are kept quite long, such as hundreds or thousands of hours. In this regard, 60 kV ($5*U_0$) and 36 kV ($3*U_0$) voltages were applied to the test samples at 15-minute intervals in order to monitor the cable behavior with more frequent measurements. The experimental setup for overvoltage application is given in Figure 6. R_k resistance connected in series to the secondary of the high voltage test transformer was used to protect the secondary windings of the transformer and limit the short circuit current in the case of a possible discharge. The magnitude of the voltage applied to the cable insulation is measured with a capacitive voltage divider (C_1 and C_2) and the conversion ratio of the voltage divider is 1/1000.

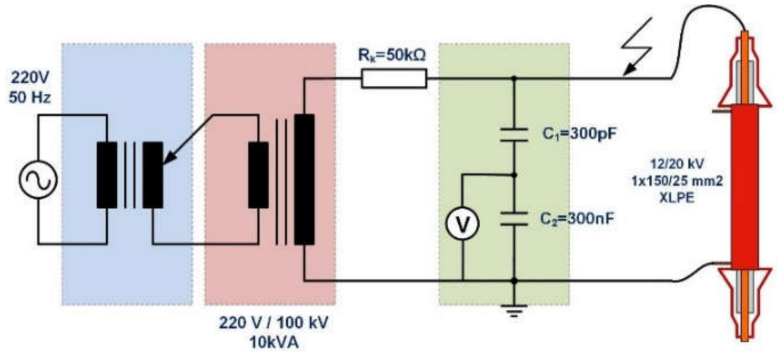


Figure 6. Experimental setup for overvoltage aging.

Detailed information on measurement methods, devices, and standards described in this section. After each aging cycle, dielectric losses (P_k), dissipation factor (tanδ), and PD were measured. The measurements were made according to the TS IEC 60502-2 standard published by the Turkish Standards Institute (TS or TSE) based on the IEC (International Electrotechnical Commission) standards. The minimum measuring voltage for the P_k and tanδ is specified as 2 kV in TS IEC 60502-2 (section 18.2.6). It is also recommended to measure the rated voltage of the cable.

In this study, dielectric losses (P_k), capacitance (C), and dissipation factor (tanδ) were measured at the 2 and 12 kV voltage and 50 Hz frequency by using the CPC100/CPTD1 measurement device as shown in Figure 7. The relative permittivity (ε_r) of the cable was examined and the behavior of the cable insulator was analyzed by using the cable capacity measurement.

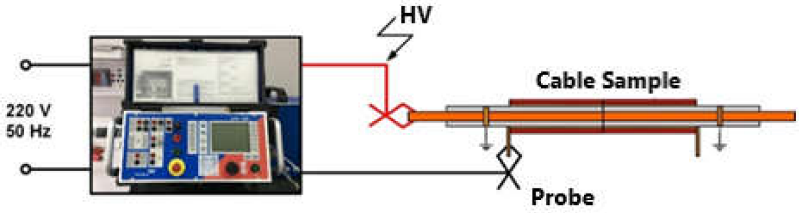


Figure 7. Omicron CPC100/CPTD1 and connection diagram.

After each aging process, PD measurements were realized by the MPD600 device as shown in Figure 8.

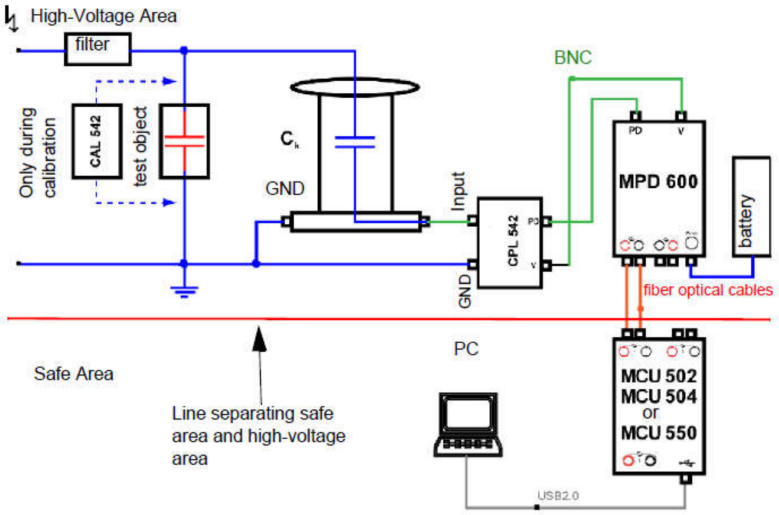


Figure 8. Omicron MPD600 and connection diagram.

The measurement method described in TS IEC 60502-2 (section 18.2.5) standard was applied exactly. In the tests, calibration of the test voltage will be provided with the calibrator unit of the MPD-600 partial discharge measurement set. Then, the voltage will be increased to $2*U_0$ in accordance with the TS IEC 60502-2 standard. After waiting for 10 seconds at the $2*U_0$ voltage level, the voltage will be reduced to $1.73*U_0$ and fixed at this level and PD measurements were carried out [26]. Measurement sensitivity ranges of the MPD 600 device are given in Table 1.

Table 1. Measurement uncertainty ranges of the MPD600 device [27].

Parameter	Sensitivity
Voltage	±0.005%
Frequency	±1ppm
PD Level	±2%

5. Measurement Results and Evaluation

In this section, measurement results are evaluated to see the effect of aging with overvoltage on MV cable and termination. Dielectric parameters and PD were measured after each aging cycle. Four cable samples were named as A, B, C, and D, and the average value of the measurement results of the two samples is indicated as MEAN. While samples A and B were aged at 60 kV, samples C and D were aged at 36 kV voltage. The data obtained were formed in two main groups. In the first group, dielectric losses (P_k) and dissipation factor (tanδ) measurements were separated according to their voltage levels. In addition, relative permittivity (ε_r) has been calculated. In the second group, PD measurement results were introduced in magnitude for before and after aging. In addition, PD inception voltage was also evaluated. Finally, the cable termination was removed and visual examination was performed to see the damaged points.

5.1. Measurements of Dielectric Parameters

The overvoltage aging process caused breakdown on each cable sample in different cycles. sample A was broken down at the 29th cycle, sample B at the 21st cycle, sample C at the 55th cycle, and sample D at the 39th cycle. As a result of the measurements, it was seen that cable samples showed different dielectric characteristics and the overall evaluation can be made by examining the average value.

5.1.1. Dielectric Losses (P_k)

It has been observed that after each aging cycle, dielectric losses increase compared to the pre-aging situation. The results of measurements of P_k at 2 and 12 kV, and 50 Hz frequency can be seen in Figure 9.

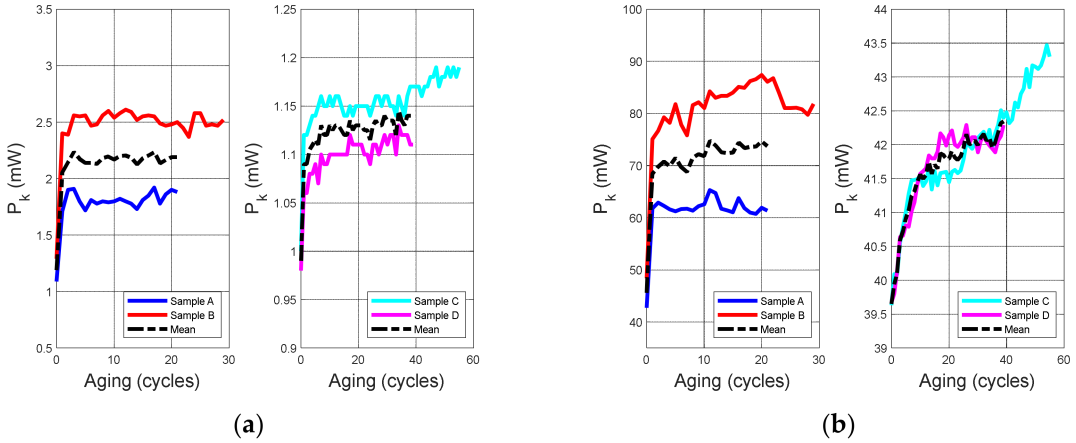


Figure 9. Dielectric loss (P_k) measurement results for 50 Hz (**a**) 2 kV and (**b**) 12 kV.

In the measurements performed at 12 kV, P_k in sample A increased by 34%, while sample B increased by 79%. However, since the cable samples behave differently, the evaluation of the average P_k value would be more accurate. There is a 62% increase in the average P_k value, calculated using the measurement results after 21 aging processes. In addition, after 39 aging cycles, the average P_k change in samples C and D was 13%.

The reason for this increase in the beginning phase of the aging process is that the bonds between PE molecules are exposed to electrical stress, which leads to them becoming stretched, and results in dielectric losses [28–32]. This increase shows that the overvoltage process stresses the cable and P_k increases. In addition, cable samples were able to withstand different number of aging processes and became unusable. It is clear that this may be the result of differences in the assembly of the cable termination.

5.1.2. Dissipation Factor (Tanδ)

The dissipation factor (tanδ) measurement results were examined to see how the electrical insulation quality of the system consisting of cable and cable head was affected by overvoltage. Tanδ measured after each aging cycle is introduced in Figure 10.

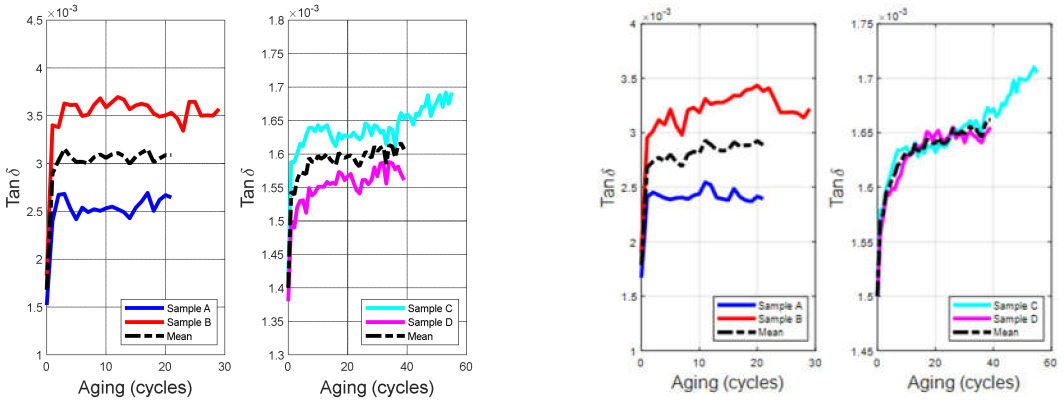


Figure 10. Tanδ measurement results for 50 Hz (**a**) 2 kV and (**b**) 12 kV.

Before the aging process, the average tanδ value of samples A and B was obtained as 0.18%. From the first aging cycle, the rate of increase in tanδ was quite rapid and reached 0.268% in the 2nd cycle. From the 2nd to the 21st cycle, the rate of increase decreased and reached 0.290%. Unlike samples A and B, the rate of average tanδ value for samples C and D increased 10% form the first aging cycle to the 20th. It maintained its condition throughout 20 aging cycles and increased its rate of increase again after the 40th aging cycle. While the average tanδ value increased by 60% in cables aged with 60 kV, the increase rate was 13% in cables aged with 36 kV.

5.1.3. Relative Permittivity (ε_r)

The relative permittivity (ε_r) measurement could not be done, but the cable capacity value was measured and the ε_r value was calculated using geometric capacitance. Detailed information about the formulation and the result obtained is calculated in Equations (7) and (8) [21].

$$\varepsilon_r = \frac{C_p}{C_0} \tag{7}$$

$$C_0 = \frac{2.\pi.\varepsilon_0.\varepsilon_{air}.l}{\ln \frac{r_2}{r_1}} \tag{8}$$

In the above equations, C_0 is the geometric capacitance (F), C_p is the measured capacitance (F), ε_0 is the relative permittivity of space and ε_{air} is the relative permittivity of air, l is the cable length (m), r_2 is the outer radius of insulation (mm), and r_1 is the inner radius of the insulation (mm). The geometric capacitance value (C_0) for the measured cable was calculated as 254.18 pF.

The change in relative permittivity value due to the aging cycle is shown in Figure 11. It is clear that the relative permittivity value calculated based on the measurements performed at 12 kV and 50 Hz, showed a slight increase as aging cycles increased.

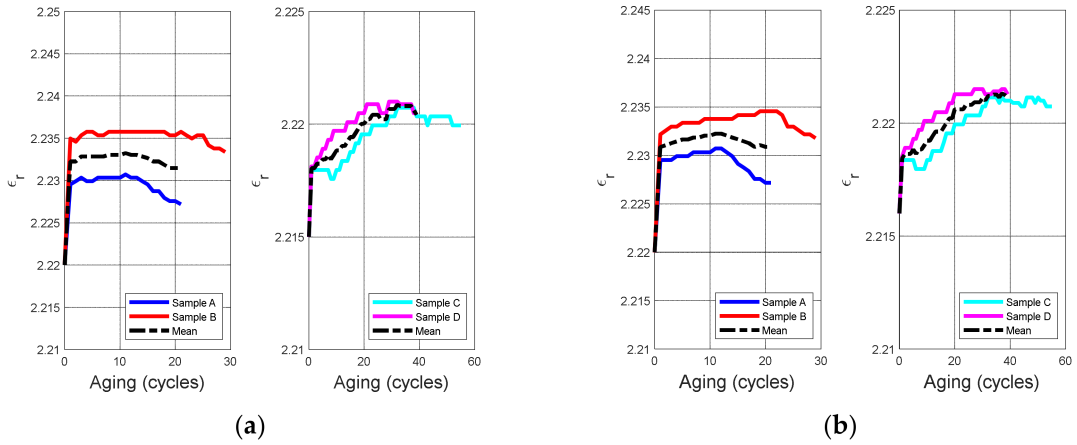


Figure 11. Relative permittivity (ε_r) at 50 Hz and (**a**) 2 kV and (**b**) 12 kV.

It is understood that the relative permittivity value shows a different increase in each sample like other dielectric parameters. Although the increased rate in samples A and B varies between 4 and 7 per thousand, the average increase value is calculated as 5.5 per thousand. For samples C and D, the average rate of change is calculated as 1.5 per thousand. It can be said that this rate of change is remarkable in measurements made at a frequency of 50 Hz.

5.2. Measurements of Partial Discharge

In this section, Figure 12 shows PD magnitude measurement results for cable samples, respectively, before and after aging. All measurements were performed in the range of 100 to 400 kHz using the "Set for IEC 60270 compliance" command on the MPD600 control screen.

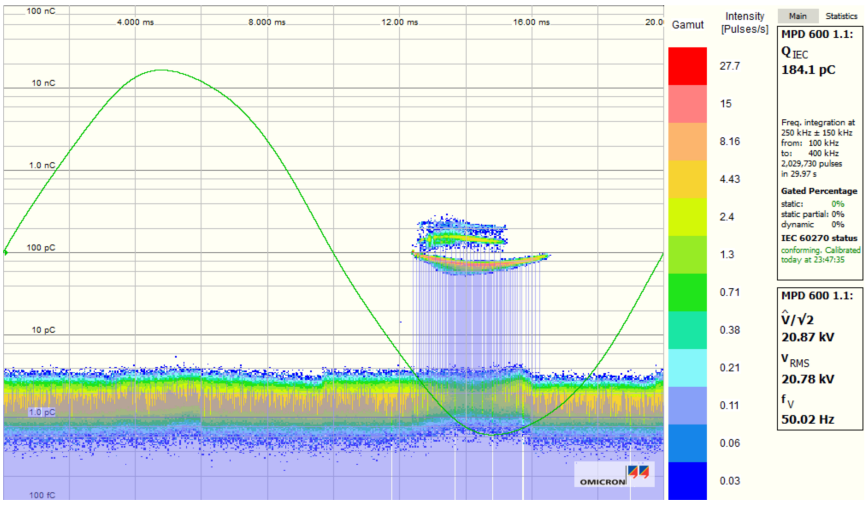
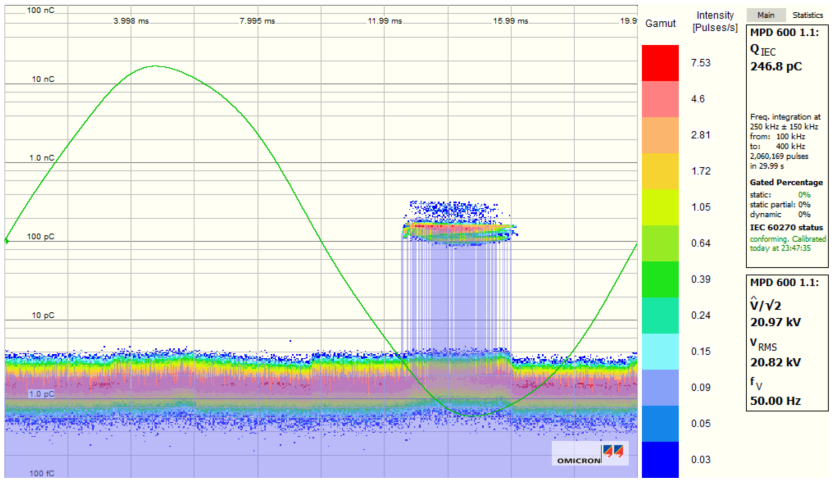


Figure 12. *Cont.*



(**b**)

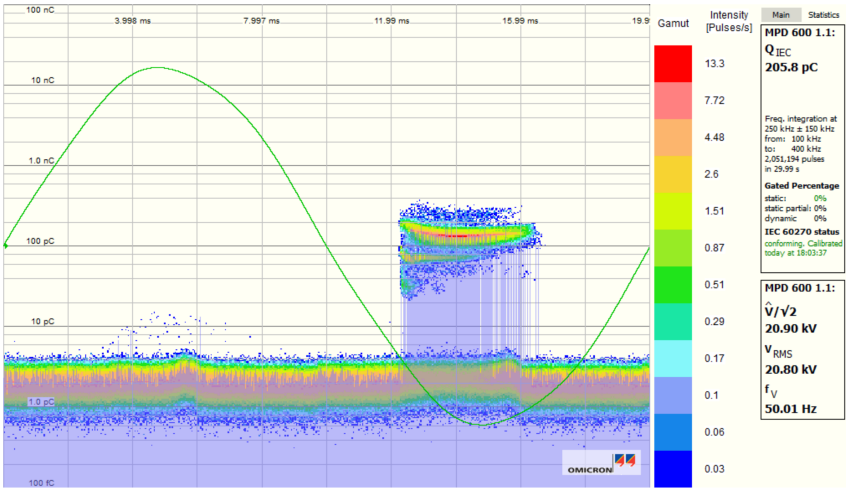
Figure 12. PD measurement results of sample A: (**a**) before and (**b**) after the 21st aging.

Sample A broke down at 29 cycles, sample B at 21 cycles, sample C at 55 cycles, and sample D at 39 cycles. In order to see the PDs caused by our measurement system and grid, the graphs were created on a scale of 100 fC to 100 nC. In the measurements made at 20.8 kV voltage and 50 Hz frequency, the PD value before the aging process was measured between 900 fC and 1 pC.

After the aging process, was a slight increase in PD events in sample A. The PD value was 185 pC before aging and it exceeded 246 pC just before the cable termination was damaged after aging. The PD measurement results of sample A are displayed in Figure 12.

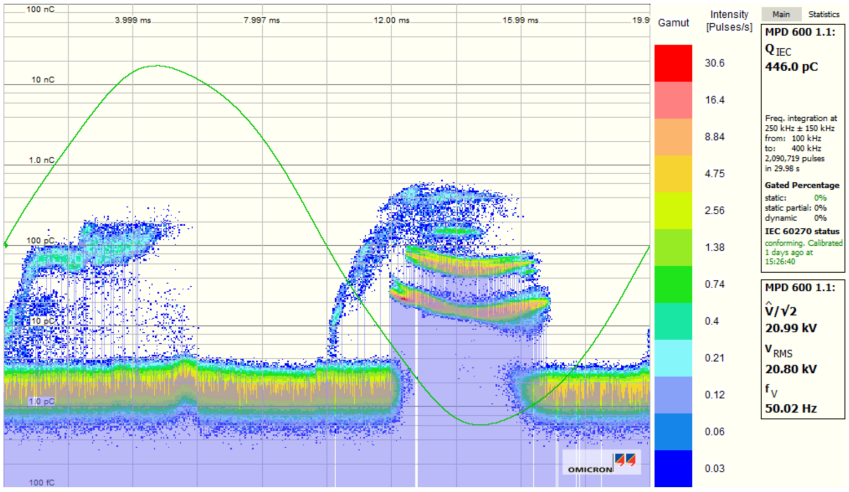
It was noticed that in the measurement of PD for sample B before aging, there were a large number of PD activities that may result from test setup or cable termination assembly as in Figure 13. The PD value, which increased from 205 to 446 pC, indicated the degradation of the cable termination of the aging process with overvoltage.

Considering that sample C was aged with a 36-kV overvoltage, the PD measurement result before aging was 60 pC, while it was 285 pC after 55 aging processes. It was seen that the increase in PD events was quite high as shown in Figure 14. The reason for this situation could be shown as the heating operation damaging the cable termination while the termination assembly was being installed.



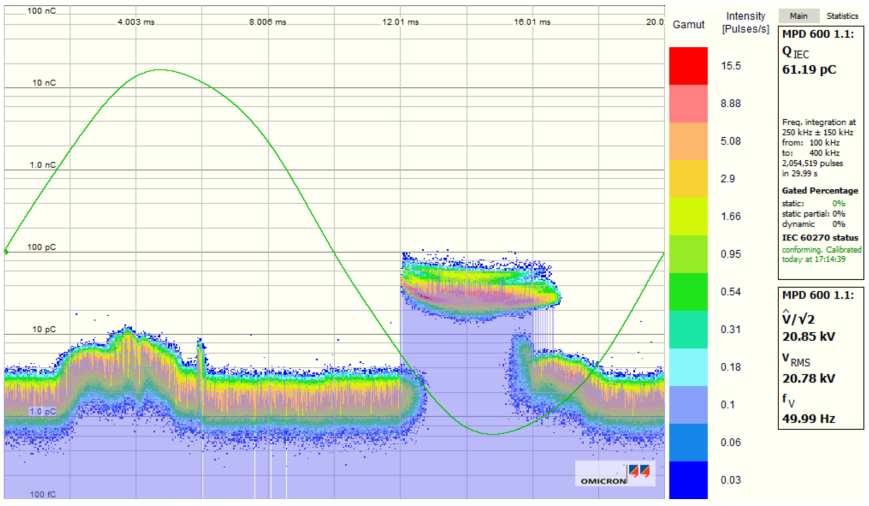
(**a**)

Figure 13. *Cont.*

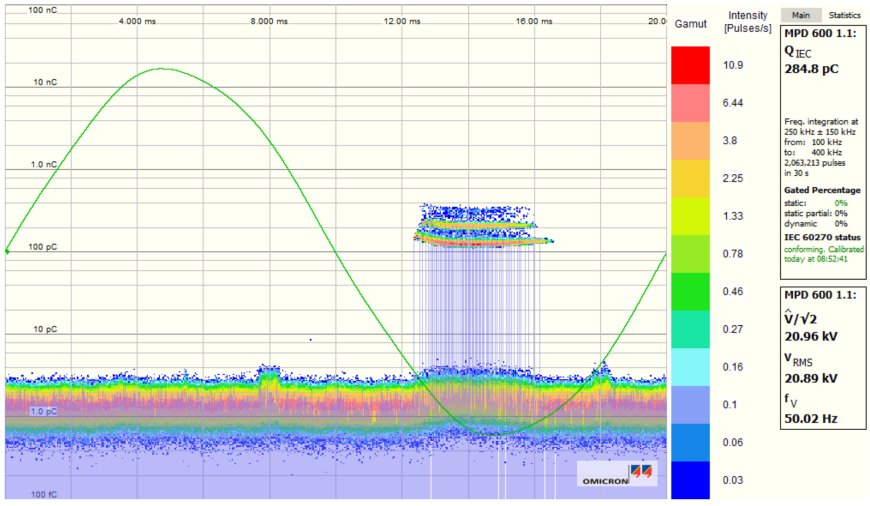


(**b**)

Figure 13. PD measurement results of sample B: (**a**) before and (**b**) after the 29th aging.



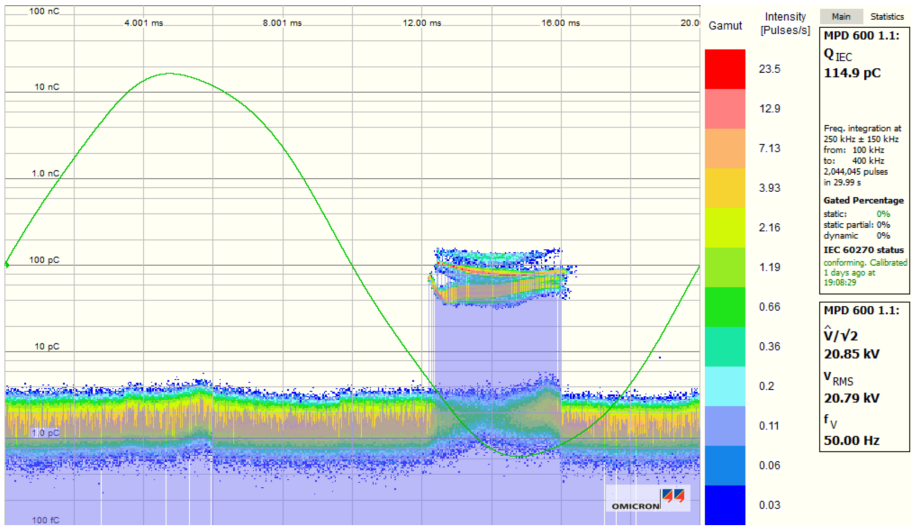
(**a**)



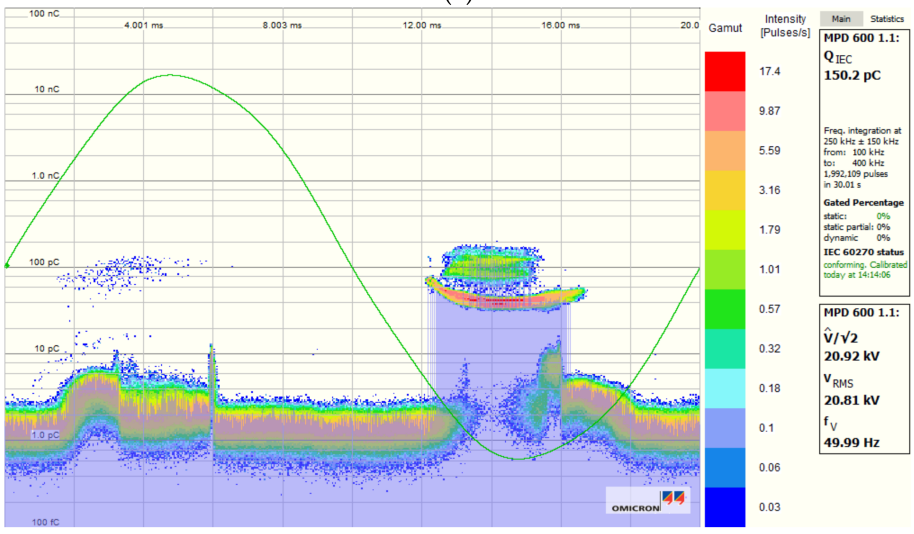
(**b**)

Figure 14. PD measurement results of sample C: (**a**) before and (**b**) after the 55th aging.

When the measurement results of sample D were examined (Figure 15), it was seen that while PD occured at a magnitude of 115 pC, it increased to 150 pC after 39 aging processes. This change in sample D met the expected results as it was aged with a 36-kV voltage.



(**a**)



(**b**)

Figure 15. PD measurement results of sample D: (**a**) before and (**b**) after the 39th aging.

When evaluating the below measurement results, it is necessary to carefully consider the definitions of PD. PDs occurring on the positive or negative rising edge of the voltage, are internal PDs. PDs occurring around the positive or negative peak of the voltage are surface discharge in the cable lug or cable termination. Surface discharges can occur in a void at cable termination for various reasons.

For example, if the inner surface of the termination is assembled with a contaminant on the surface, this can cause the surface stress to initiate surface discharges. Normally, this occurs in the region of the stress cone due to the highest transverse electric field. Another cause for surface discharges is poor preparation and workmanship.

Based on the information obtained from the studies performed using different aging methods in the literature, it can be predicted that the inception voltage value of the PDs in the cable system will decrease. However, the most important point to be noted here is that errors occurring in the assembly of the cable termination affect the PD amplitude rather than the PD inception voltage. Details can be seen in Figure 16.

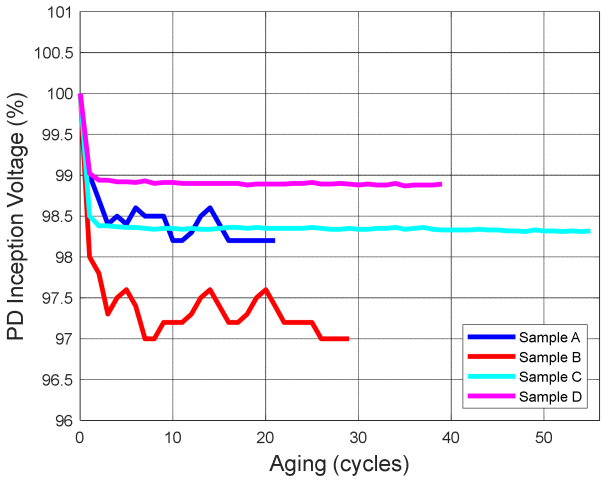


Figure 16. PD inception voltage measurement results at 20.8 kV.

5.3. Defects Occurring in the Cable Termination

The cables were aged using overvoltage broken down in a different number of aging cycles. Breakdown occurred under the stress-relief material of the cable termination. The details are shown in Figure 17. It was observed that the failure that occurred in different cable samples was not in the cable insulation but in the cable termination. We can determine the actual status of the cable and cable termination with dielectric parameters and partial discharge measurements. One or more of the reasons, such as an air gap or contamination that may occur during the assembly of the cable termination, the incomplete scraping of the semiconductor surface, or improper placement of the stress-relief material, can lead to this situation. In addition, the reason for this situation can be explained as the heating process damaging the cable termination during the termination assembly installation.



Figure 17. Breakdown location in the cable termination.

6. Discussion

In this study, the behavior of the cable and the faults caused by the defects that may occur in the termination of the cable under overvoltage has been examined. The effectiveness of different dielectric diagnostic methods has been studied. Four test samples were created from 12/20.8 kV XLPE insulated cable using the equipment at the Yildiz Technical University High Voltage Laboratory and were aged with overvoltage using three times ($3*U_0$) and five times ($5*U_0$) the rated voltage. The results and considerations in this study can be presented as follows.

In the dielectric analysis of the cable, it was seen that the measurement of dielectric parameters can only give an idea about the cable, and these measurements are insufficient when it comes to cable

termination. In measurements made at the rated frequency, the tanδ value can be used as characteristic data to learn the aging degree of the cable. However, this situation is not valid for relative permittivity (ε_r). It has been observed that an increase in P_k in cables aged at different overvoltage values do not give a clear idea about the cable life. On the contrary, it is necessary to examine these data in detail with numerical analysis methods and with more cable samples. In addition, it is quite clear that when an increase in dielectric parameters of 40% and above occurs, closer monitoring of the cable is required.

In PD measurements, similar trends were observed for each cable sample. The type of PD indicates poor workmanship in cable termination assembly. In the measurements, there was a breakdown of the stress relief material. The results of PD the measurement are consistent with this situation. It is concluded that PD measurement plays a more effective role than tanδ for diagnosing the cause and location of cable termination failure.

Although cable samples were formed from the same cable type, they were broken down at different aging cycles. In this context, another conclusion is that defects that may occur during the preparation of cable samples can be considered as poor workmanship. The effect of even the smallest error in the heat treatment applied during the assembly of the cable termination on the life of the termination has been clearly demonstrated. However, the most important point to be addressed in this regard is that workmanship mistakes are not made consciously. When the measurement results were examined, it was concluded that they give information about the increase in the probability of failure and the shortening of the life of the cable system. Measuring of PDs after the cable termination assembly process will contribute to the reduction of energy cuts and prevent economic losses.

In future studies, it is planned to cause aging with different methods, to make measurements at different frequencies, and to work with different cable samples.

Author Contributions: C.C.U. and O.A. worked on conceptualization, methodology, measurement, validation, formal analysis, writing—original draft preparation, writing—review and editing. All authors have read and agreed to the published version of the manuscript.

Funding: This research was funded by Scientific Research Project Coordinator of Yildiz Technical University grant number FDK-2020-3897 and the APC was funded by authors.

Acknowledgments: Scientific Research Project Coordinator of Yildiz Technical University supported this research study with the project number FDK-2020-3897. The authors would like to thank the Yildiz Technical University for financial support.

Conflicts of Interest: The authors declare no conflict of interest.

References

1. Lowczowski, K.; Lorenc, J.; Tomczewski, A.; Nadolny, Z.; Zawodniak, J. Monitoring of MV Cable Screens, Cable Joints and Earthing Systems Using Cable Screen Current Measurements. *Energies* **2020**, *13*, 3438. [CrossRef]
2. Zhan, Y.; Chen, G.; Hao, M.; Pu, L.; Zhao, X.; Wang, S.; Liu, J. Space charge measurement and modelling in cross-linked polyethylene. *Energies* **2020**, *13*, 1906. [CrossRef]
3. *IEEE Guide for Field Testing and Evaluation of the Insulation of Shielded Power Cable Systems Rated 5 kV and Above*; IEEE Std 400-2012 (Revision of IEEE Std 400-2001); IEEE: Piscataway, NJ, USA, 2012. [CrossRef]
4. Chimunda, S.; Nyamupangedengu, C. A reliability assessment model for an outdoor 88 kV XLPE cable termination. *Electr. Power Syst. Res.* **2019**, *177*, 105979. [CrossRef]
5. Souza, R.E.; Silveira, F.H.; Gomes, R.M.; Lima, G.S.; De Conti, A.; Visacro, S. Characterization of the effect of the insulating material of covered cables on the impulse breakdown behavior of single- and three-phase compact distribution lines. *Electr. Power Syst. Res.* **2019**, *172*, 161–166. [CrossRef]
6. Grzybowski, S.; Cao, L.; Pushpanathan, B. Electrical accelerated aging of EPR cable insulation energized by AC voltage and switching impulses. *Annu. Rep. Conf. Electr. Insul. Dielectr. Phenom. CEIDP* **2009**, 51–54. [CrossRef]
7. Mladenovic, I.; Weindl, C. Artificial aging and diagnostic measurements on medium-voltage, paper-insulated, lead-covered cables. *IEEE Electr. Insul. Mag.* **2012**, *28*, 20–26. [CrossRef]

8. Mecheri, Y.; Nedjar, M.; Lamure, A.; Aufray, M.; Drouet, C. Influence of moisture on the electrical properties of XLPE insulation. *Annu. Rep. Conf. Electr. Insul. Dielectr. Phenom. CEIDP* **2010**, 1–4. [CrossRef]
9. Mecheri, Y.; Medjdoub, A.; Boubakeur, A.; Boujemaa, S. Characterization of laboratory aged MV XLPE cables using dielectric losses factor measurements. In Proceedings of the 2014 International Conference on Electrical Sciences and Technologies in Maghreb (CISTEM), Tunis, Tunisia, 3–6 November 2014. [CrossRef]
10. Cao, L.; Grzybowski, S. Accelerated aging study on 15 kV XLPE and EPR cables insulation caused by switching impulses. *IEEE Trans. Dielectr. Electr. Insul.* **2015**, *22*, 2809–2817. [CrossRef]
11. Cao, L.; Zanwar, A.; Grzybowski, S. Electrical aging phenomena of medium voltage EPR cable energized by ac voltage with switching impulses superimposed. In Proceedings of the 2011 IEEE Electric Ship Technologies Symposium, Alexandria, VA, USA, 10–13 April 2011; pp. 353–356. [CrossRef]
12. Dabbak, S.Z.; Illias, H.A.; Ang, B.C. Effect of surface discharges on different polymer dielectric materials under high field stress. *IEEE Trans. Dielectr. Electr. Insul.* **2017**, *24*, 3758–3765. [CrossRef]
13. Knenicky, M.; Prochazka, R.; Hlavacek, J. Partial Discharge Patterns during Accelerated Aging of Medium Voltage Cable System. In Proceedings of the 2018 IEEE International Conference on High Voltage Engineering and Application (ICHVE), Athens, Greece, 10–13 September 2018; pp. 3–6. [CrossRef]
14. Eigner, A.; Rethmeier, K. An overview on the current status of partial discharge measurements on AC high voltage cable accessories. *IEEE Electr. Insul. Mag.* **2016**, *32*, 48–55. [CrossRef]
15. Long, X.; Liu, J.; Zhao, X.; Li, J.; Chen, X.; Zhao, A.; Deng, J.; Zhang, G. The degradation of 10kV XLPE cable accessories under switching impulses. *Proc. IEEE Int. Conf. Prop. Appl. Dielectr. Mater.* **2018**, 463–466. [CrossRef]
16. Wu, J.; Heredia, L.C.C.; Mor, A.R.; Smit, J.J. Partial Discharges at Artificial Defects in XLPE Cable Accessories under Superimposed Transients. In Proceedings of the 2018 IEEE International Conference on High Voltage Engineering and Application (ICHVE), Athens, Greece, 10–13 September 2018; pp. 4–7. [CrossRef]
17. Ghaderi, A.; Mingotti, A.; Lama, F.; Peretto, L.; Tinarelli, R. Effects of temperature on mv cable joints tan delta measurements. *IEEE Trans. Instrum. Meas.* **2019**, *68*, 3892–3898. [CrossRef]
18. Ghaderi, A.; Mingotti, A.; Peretto, L.; Tinarelli, R. Effects of Mechanical Pressure on the Tangent Delta of MV Cable Joints. *IEEE Trans. Instrum. Meas.* **2019**, *68*, 2656–2658. [CrossRef]
19. Cichecki, P. Testing and Diagnosis of High Voltage and Extra High Voltage Power Cables with Damped AC Voltages. 2018. Available online: https://doi.org/10.4233/uuid:f50c2129-6771-468b-aa3c-7c1fdac4e425 (accessed on 21 April 2020).
20. Available online: https://www.te.com/usa-en/product-CAT-OXSU.datasheet.pdf (accessed on 21 April 2020).
21. Kreuger, F.H. *Industrial High Voltage Part: 1–6*; Delft University Press: Delft, The Netherlands, 1992; ISBN 90-6275-562-3.
22. Kumru, C.F. Experimental Investigation on Dielectric Loss Parameters of High Voltage Cables in Various Operational Conditions Using Artificial Neural Networks. Ph.D. Thesis, Department of Electrical Engineering, Yildiz Technical University, Istanbul, Turkey, 2016.
23. IEC 60270. *High-Voltage Test Techniques-Partial Discharge Measurements, International Standard*; IEC: Geneva, Switzerland, 2000.
24. Wadhwa, C.L. *High Voltage Engineering*, 2nd ed.; New Age International Private Limited: New Delhi, India, 2007.
25. Smith, C. *Partial Discharge and Insulation Failure*; Independent Power Engineering Consultants (IPEC) Ltd.: Manchester, UK, 2005.
26. TS IEC 60502-2. *Power Cables with Extruded Insulation and Their Accessories for Rated Voltages from 1 kV (Um = 1,2 kV) Up to 30 kV (Um = 36 kV)—Part 2: Cables for Rated Voltages from 6 kV (Um = 7,2 kV) Up to 30 kV (Um = 36 kV)*; IEC: Geneva, Switzerland, 2015.
27. *Omicron MPD 600 User Manual Omicron MPD 600 User Manual*; OMICRON Electronics GmbH: Klaus, Austria, 2011.
28. Boukezzi, L.; Rondot, S.; Jbara, O.; Boubakeur, A. Study of thermal aging effects on the conduction and trapping of charges in XLPE cable insulations under electron beam irradiation. *Radiat. Phys. Chem.* **2018**, *149*, 110–117. [CrossRef]
29. Taslak, E.; Arikan, O.; Kumru, C.F.; Kalenderli, O. Analyses of the insulating characteristics of mineral oil at operating conditions. *Electr. Eng.* **2018**, *100*, 321–331. [CrossRef]

30. Das-Gupta, D.K.; Scarpa, P.C.N. Polarization and dielectric behavior of ac-aged polyethylene. *IEEE Trans. Dielectr. Electr. Insul.* **1996**, *3*, 366–374. [CrossRef]
31. He, D.; Gu, J.; Wang, W.; Liu, S.; Song, S.; Yi, D. Research on mechanical and dielectric properties of XLPE cable under accelerated electrical-thermal aging. *Polym. Adv. Technol.* **2017**, *28*. [CrossRef]
32. Kumru, C.F.; Arikan, O.; Kocatepe, C.; Kalenderli, O. Investigation of Effect of Temperature Variation in a High Voltage Cable on Electrical Insulation. In Proceedings of the 18th International Symposium on High Voltage Engineering, Seoul, Korea, 25–30 August 2013; pp. 1104–1109.



© 2020 by the authors. Licensee MDPI, Basel, Switzerland. This article is an open access article distributed under the terms and conditions of the Creative Commons Attribution (CC BY) license (http://creativecommons.org/licenses/by/4.0/).